ACS Energy Letters **2017**, *2*, 549-555

https://doi.org/10.1021/acsenergylett.7b00047

Electrochemical Reduction of Carbon Dioxide to Methanol in the Presence of Benzannulated Dihydropyridine Additives

Patrick K. Giesbrecht[a] and David E. Herbert[a,b]*

[a]*Department of Chemistry and* [b]*Manitoba Institute for Materials, University of Manitoba, 144 Dysart Rd, Winnipeg, MB, Canada R3T 2N2*

ABSTRACT: Dihydropyridines (DHPs) have been postulated as active intermediates in the pyridine-mediated electrochemical conversion of CO_2 to methanol, however the ability of isolated DHPs to facilitate methanol production in a similar fashion to their parent aromatic *N*-heterocycles (ANHs) has not been tested. Here, we use bulk electrolysis to show that 1,2- and 1,4-DHPs (1,2-dihydrophenanthridine and 9,10-dihydroacridine) can mediate the sub-stoichiometric electrochemical reduction of CO_2 to methanol and formate with similar Faradaic efficiencies as the corresponding ANHs at Pt electrodes. 1,2-dihydrophenanthridine furthermore exhibits improved CO_2 reduction activity compared to its parent ANH (phenanthridine) at glassy carbon electrodes. These results provide the first experimental evidence for the participation of DHPs as additives in electrochemical CO_2 reduction.

TOC GRAPHIC

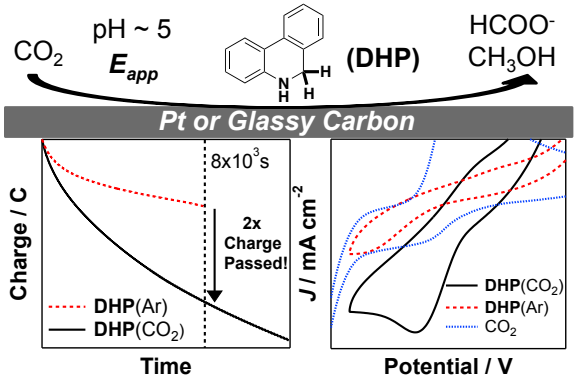

The recycling of CO_2 directly to liquid chemicals using water and a renewable energy source is a promising route to sustainable carbon-based fuels.[1-2] Reports that the addition of simple aromatic *N*-heterocycles (ANHs) such as pyridine (**1**) leads to the production of methanol in acidic aqueous electrochemical[3-6] and photochemical[7-11] cells at low overpotentials or light-driven underpotentials have garnered both justifiable excitement[12] and a healthy amount of scrutiny.[13-14] Recent studies[10,15-17] have verified that methanol is indeed produced and only in the presence of ANH additives, but also that multi-e^-/multi-H^+ reduced products such as methanol and formic acid are generated with low, sub-stoichiometric turnover numbers (TONs; 0.04-0.33) with product selectivity and Faradaic efficiencies (%FE) dependent on the nature of the electrode used.[3-4,7-8,15,18-19]

Given the promise of this simple system, the role of the ANH additive, the acidic solution and the electrode surface in the overall mechanism have been subject to on-going debate. Computational studies from Carter, Musgrave, and furthered by Keith, suggest a critical role for $2e^-/2H^+$ reduced dihydropyridines (DHPs) as intermediates (Figure 1),[20-23] either formed in solution[22] or adsorbed to the electrode surface.[20,24] A 'weak-acid mechanism'[13,25] has also been proposed where the conjugate acid of the ANH additive is reduced at the electrode surface to form adsorbed hydrogen, H_{ads}, which then participates in proton-coupled hydride transfer (PCHT) with a second equivalent of $[ANH\text{-}H]^+$ to facilitate CO_2 reduction[26-27] but can also participate in hydrogen evolution.

Despite their prominence in computed mechanisms, the ability of isolated DHPs themselves to facilitate methanol production in a similar fashion to parent ANHs has to date not been tested. We hypothesized that if DHPs are competent intermediates, they should exhibit comparable activities to their parent ANHs. We therefore screened isolated

DHPs [1,2-dihydrophenanthridine (**3-H₂**) and 9,10-dihydroacridine (**4-H₂**)] as additives in electrochemical CO_2 reduction at both Pt and glassy carbon electrodes.

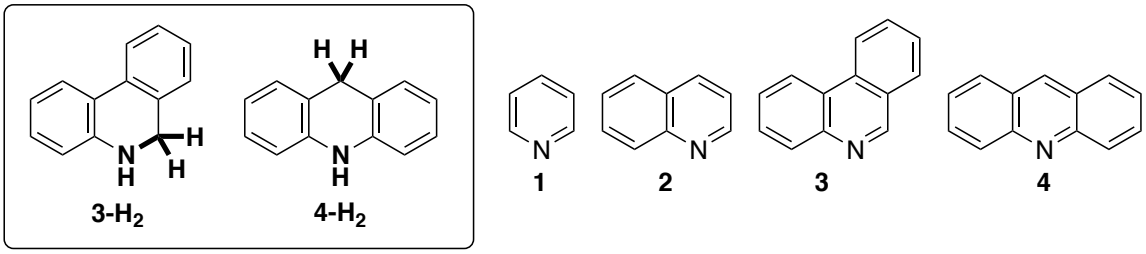

Figure 1. Structures of DHPs and related ANHs studied as additives in this work.

DHPs **3-H₂** and **4-H₂** are chemically similar to the 1,2- and 1,4-DHP isomers of **1-H₂** proposed as intermediates in pyridine-mediated CO_2 reduction (Figure 1). While a purely aqueous electrochemical system is more ideal for fuel-forming purposes, a mixed aqueous/organic solvent system was utilized here for solubility reasons.[28] Accordingly, we also evaluated the activities of the parent ANHs phenanthridine (**3**; 3,4-benzoquinoline) and acridine (**4**; 2,3-benzoquinoline), as well as those of pyridine (**1**) and quinoline (**2**) in this mixed solvent system to enable comparisons with DHPs **3-H₂** and **4-H₂**.

Bulk electrolyses were conducted to quantify yields of liquid fuel candidates methanol and formate.[29] Potentiostatic electrolyses were used to ensure selectivity of the reductive processes, with $E_{applied}$ and the charge passed chosen based on previously reported optimizations for **1**[17] with a shift in the potential scale vs $Fc^{0/+}$ due to the use of a mixture of solvents taken into account for accurate comparison of $E_{applied}$.[30] The $E_{applied}$ = -0.75 V vs $Fc^{0/+}$ used for experiments at Pt is at the onset of the reduction peak observed by CV for all the ANHs under CO_2 (Figure 3), while for reticulated vitreous carbon (RVC) electrodes $E_{applied}$ = -1.20 V vs $Fc^{0/+}$, at the onset of the reduction peaks observed in CVs

for **1-3** at GCEs (Figure S9). Potentials were applied for *ca.* 10 000 s (see SI for CPE curves), with multiple analytical techniques (^{1}H NMR, GC-MS, GC-FID and LC-MS; see SI for experimental details and integration methods) employed to corroborate identification of specific organic products. Care was taken to address the potential for contamination during sample preparation and analysis (see SI).[14]

From the GC and LC traces (see SI for chromatograms), the absolute yields of products obtainable under the conditions employed are low (10-250 μM methanol and/or formate), consistent with absolute amounts observed in previous reports measuring the activity of **1** in aqueous electrochemical cells.[3-4,7-8,15,17-18] As a result, the TONs we report for this system are sub-stoichiometric relative to the amount of DHP/ANH added (Table 1), in line with the literature on **1**. The accuracy of the analytical techniques employed was checked using standard solutions, and the precision evaluated by running samples in triplicate and over a span of three months. The largest component of the error in our reported values based on GC-FID is attributed to sample-to-sample reproducibility in bulk electrolysis rather than the detection limit or consistency of the instruments used. ^{1}H NMR (~3.24 ppm, see SI) and GC-MS corroborated the identification of methanol. The LC-MS method used for formic acid quantification proved less sensitive, and as such larger corresponding errors were determined for the reported values.

For DHPs **3-H$_2$** and **4-H$_2$**, %FEs determined from bulk electrolysis experiments at Pt are comparable with those observed for parent ANHs **3** and **4** (Table 1). Analysis of the electrolyzed reaction mixture by ^{1}H NMR showed that ~40% of **3-H$_2$** is converted to **3** after CO_2 reduction at Pt surfaces (Figure S19), with similar conversion of **4-H$_2$** to **4** under the same conditions. In comparison, potentiostatic electrolysis of **3-H$_2$** at the same

pH under Ar (in the absence of CO_2) resulted in an order of magnitude lower conversion of **3-H₂** to **3** (Figure S26), and 50% less charge passed compared to under CO_2 (Figure 2a). This is consistent with the majority of the reactivity of the DHP and charge passed attributable to reaction of the DHP with CO_2. The observed methanol and formic acid are therefore not simply products of an ANH-mediated process resulting from conversion of the DHP to its parent ANH under the conditions employed.

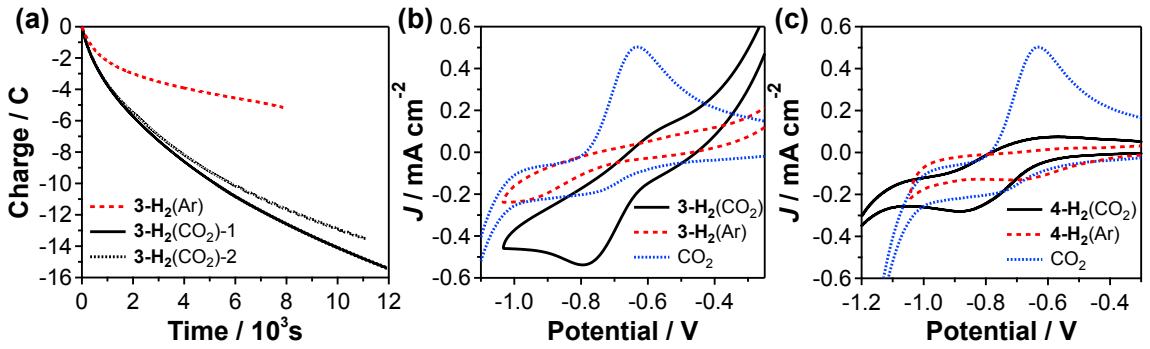

Figure 2. (a) Charge passed in bulk electrolyses of 10 mM **3-H₂** ($E_{applied}$ = -0.75 V vs $Fc^{0/+}$, Pt mesh electrode) under Ar (red dash) and two separate runs under CO_2 (black traces); comparison of CVs of 10 mM **3-H₂** (b) and **4-H₂** (c) under Ar at pH = 5.5 and under CO_2 (black) with CO_2 alone (blue), ν = 100 mV/s; 0.1 M $LiClO_4$ in CH_3CN/H_2O (40% v/v), Pt disc; *E* vs $Fc^{0/+}$.

Furthermore, electrolysis of **3-H₂** at RVC also led to methanol and formate production with similar %FE as seen at Pt electrodes, and with higher %FE than observed for **3**. This demonstrates that isolated DHPs can function as additives in a similar fashion to their parent ANHs, which is consistent with the proposed role of DHPs as intermediates relevant in ANH-mediated reduction of CO_2 to methanol.[21-24] No reduced products were detected when electrolysis of **3-H₂** under CO_2 was performed at a lower potential (-0.75 V vs. $Fc^{0/+}$) at RVC electrodes.

Table 1. Faradaic efficiencies for electrochemical CO_2 reduction in the presence of DHP or ANH additives

Additive	Electrode	%FE[a] CH_3OH	%FE[b,c] $HCOO^-$	TON CH_3OH (10^{-3})	TOF CH_3OH (10^{-3} hr^{-1})	TON $HCOO^-$ (10^{-3})	TOF $HCOO^-$ (10^{-3} hr^{-1})
1	Pt	30(10)	not det.	12.0(1.0)	4.3(4)	-	-
1	RVC	7(7)	1.0(0.3)	0-4	0-1	0.76(24)	0.27(8)
2	Pt	36(16)	4(6)	15(7)	5.2(2.7)	6.6(9)	2.1(4)
2	RVC	11(7)	4(3)	3.9(1.9)	1.4(9)	0.8-20	0.2-5
3	Pt	12(8)	4(1)	7(3)	2.5(1.2)	5.4(1.0)	1.9(4)
3	RVC	5(3)	1.1(0.2)	2.2(1.6)	0.8(6)	1.56(22)	0.54(19)
3-H_2	Pt	19(7)	3(4)	9(3)	1.9(5)	0-8	0-2
3-H_2	RVC	15(7)	8(3)	4.3(2.4)	1.3(6)	5.9(2.2)	1.9(8)
4	Pt	17(13)	not det.	6(4)	2.1(1.6)	-	-
4	RVC	-[d]	-[d]	-	-	-	-
4-H_2	Pt	13(10)	not det.	4(3)	1.2(9)	-	-
4-H_2	RVC	-[d]	-[d]	-	-	-	-

[a]Via peak area of GC-FID traces (see SI) with standard deviation of bulk electrolysis samples. [b]Via peak area from LC-MS traces (see SI). [c]Signals for ANH overlap with product signals in ^1H NMR. [d]Significant electrode fouling (deposition).

Turning to the ANHs themselves, CO_2 reduction in the presence of an ANH additive was also seen at more inert electrode surfaces (RVC) at more reducing potentials.[31] **1**-**3** all exhibit a significant drop in %FE going from Pt to RVC electrodes with no products detected at a lower $E_{applied}$ (-0.75 V vs. $Fc^{0/+}$; RVC). The %FEs determined in this work for **1** are slightly higher, though not statistically different within error, than %FEs found reported for aqueous cells in the literature, though we note that in a mixed organic/aqueous solvent system CO_2 is expected to be more soluble,[32] and direct comparisons to literature %FEs should be made cautiously. Quinoline (**2**), recently proposed as a viable ANH additive on thermodynamic considerations,[33] exhibits the highest overall %FE and the highest methanol production of the series at both electrode surfaces. Pyridine (**1**) and acridine (**4**) exhibit the highest selectivity for methanol

formation, with no formate observed by ^{1}H NMR or LC-MS at Pt, indicating only trace amounts produced under our experimental conditions.

Unlike the correlation between pK_a and total Faradaic yields previously reported for a series of substituted pyridines in water,[5] the highest overall activity of **1**-**4** is observed for the ANH with an intermediate pK_a (**2**). Lower %FEs are observed for ANHs with higher (**1**, **4**) and lower (**3**) pK_a's.[34] The ease with which an ANH participates in a 'weak acid' reduction to form H_{ads} is apparently not %FE determining in our system. This agrees with the observation that acetic acid, which has a pK_a close to **[1-H]**$^+$, does not mediate methanol production.[25]

To put into context the hydride donor ability of the DHPs, Musgrave estimated the hydride nucleophilicity (*N*) of **3-H$_2$** ($N_{\mathbf{3\text{-}H2}} \sim 8.1$) to be comparable to the experimentally determined value for the well-known hydride donor Hantzsch's ester ($N = 9.00$). The experimentally determined value for 10-methyl-9,10-dihydroacridine, the *N*-methyl derivative of **4-H$_2$**, is $N = 5.54$, while the 1,2-isomer of **1-H$_2$** is estimated to be the strongest DHP hydride donor ($N \sim 11.4$).[22] The hydride nucleophilicity of *ortho*-1,2-dihydroquinoline (**2-H$_2$**) is reasoned to be intermediate between that of *ortho*-1,2-dihydropyridine (**1-H$_2$**) and 1,2-dihydrophenanthridine (**3-H$_2$**). This is on the basis that the remaining olefinic sub-unit in the partially hydrogenated *ortho*-**2-H$_2$** retains conjugation with an intact aromatic benzo ring and is therefore stabilized with respect to the diene fragment of **1-H$_2$**. In comparison, formation of **3-H$_2$** or **4-H$_2$** leaves in tact two aromatic benzo subunits. The reactivity of the isolated C=N bond towards hydrogenation in **3** is highlighted by the fact that the 'imine-bridged, biphenyl' resonance contributor dominates the ground state structure of **3**, in accordance with Clar's postulate.[35] All have

been calculated to be competent hydride donors for CO_2 reduction based on thermodynamic considerations.[22,33] **3-H₂** has been used in the transfer hydrogenation of C=O bonds in α-ketoesters.[36-37]

Combined with the calculated or experimental hydride nucleophilicities of the rest of the series, we estimate an order of decreasing hydride donor ability from **1-H₂** > **2-H₂** > **3-H₂** > **4-H₂**. We hypothesize that if the reactivity of ANH additives **1**-**4** is via formation of a DHP, the comparably high activity of **2** is derived from a balance between the Lewis acidity of the parent ANH (ease of formation of a DHP, lower susceptibility to side reactions) and hydride donor ability of the DHP once formed. Keith has similarly proposed on the basis of quantum chemistry thermodynamic calculations that ANH-mediated multi-e^-/multi-H^+ CO_2 may be governed by the Sabatier Principle, where Brønsted acidity and hydride donor ability must be balanced to manage both H^+ and H^- transfer to CO_2.[33] While phenanthridine (**3**) and acridine (**4**) mediate reduction of CO_2 with similar %FEs, **4** additionally undergoes a more prominent deposition process (see Figure S6). Access to *ortho*- (available in **3**, not available in **4**) or *para*-positions (available in **4**, not available in **3**) likely governs the interaction of an ANH at the electrode surface. Electrochemical deposition of 1,10-phenanthroline in acid, for example, was shown to occur via covalent modification of GCE surfaces through the *para*-position of the ANH.[38-39]

The differences in %FE observed at Pt compared with RVC for the ANH series and the lower applied potential is consistent with an important role for the electrode surface in the observation of CO_2 reduction.[20-21,24,40] Nevertheless, we tested the possibility of a homogeneous reaction between CO_2 and DHPs **3-H₂** and **4-H₂** by conducting NMR scale

reactions of **3-H$_2$**/**4-H$_2$** under CO_2 (1 atm) in CD_3CN/D_2O (1:0.1 v:v) to probe the chemical reactivity in the absence of an electrode surface or applied potential. ^{1}H NMR analysis showed no observable conversion of DHP to ANH at room temperature, and no CO_2-derived products, H_2 generation, or H/D scrambling (Figures S23-S24), in agreement with reported results for **1**/**1-H$_2$** mixtures and **1** with Pt nanoparticles.[9,25] The absence of direct chemical reaction suggests that participation of the electrode surface and an applied potential is critical for CO_2 reduction mediated by a pre-formed DHP in an electrochemical system.[24,41-42]

CVs of DHPs **3-H$_2$**/**4-H$_2$** in the absence of CO_2 showed no reductive events in initial cathodic scans of neutral or acidic solutions at Pt (Figure 2b) or GCE (Figure S11). Cathodic current can be observed after cycling through a $2e^-/2H^+$ electrochemical oxidation (0.3-0.5 V vs $Fc^{0/+}$), with this new reductive event accordingly assigned to reduction of newly formed **[3-H]$^+$**/**[4-H]$^+$** (Figure S11).[43] Introduction of CO_2 results in the appearance of an irreversible reduction at -0.8 V vs $Fc^{0/+}$ when the potential is initially swept from the open circuit potential for **3-H$_2$**, with a large current enhancement compared to the initial cathodic scan under acidic conditions (Ar) and for a CO_2 saturated solution without any **3-H$_2$** present (Figure 2b). At the potentials applied in the bulk electrolysis reactions, DHPs **3-H$_2$**/**4-H$_2$** therefore only exhibit an appreciable current response by CV at the scan rates examined in the presence of CO_2. In other words, for pre-formed DHPs, all four components – **3-H$_2$**, CO_2, an electrode and a sufficiently reducing potential – are required to observe methanol production in bulk electrolysis, and current enhancement by CV.

In comparison, CVs of ANHs **1**-**4** at Pt in the absence of CO_2 but under similar acidic conditions show a quasi-reversible reduction at ~ -0.7 V vs $Fc^{0/+}$, with a scan rate dependence corresponding to diffusion control (see SI). A linear correlation is observed between $E_{1/2}$ and ANH pK_a, with a slope of -0.054 mV/[unit pH], indicating the 'weak acid' relationship observed in water[13,25] is preserved in mixed CH_3CN/H_2O (see Figure S1, Equation 1 in SI).

Introduction of CO_2 to the ANH solution results in an increase in the current observed on the CV timescale for **1-3** (Figure 3), though only for **1** and **2** is the enhancement above the sum of the background currents ($J_{ANH/[ANH-H]+} + J_{CO2}$) at the scan rates employed. In aqueous solution, increased cathodic current for solutions of **1** in the presence of CO_2 was only detected at scan rates less than 10 mVs^{-1}.[44] For **3**, the enhancement is not significant compared to the sum of the background currents ($J_{\mathbf{3}/[\mathbf{3}\text{-}\mathbf{H}]+} + J_{CO2}$; Figure 3c).[13,19] At the scan rates employed (100 mV/s), this current enhancement is likely a result of the presence of dissolved CO_2/H_2CO_3 in solution as described previously.[13,44] In a recent study, Rybchenko et al. confirmed that, in addition to methanol production, hydrogen evolution is the dominant electrochemical reaction in **1**-containing aqueous electrolyte solution at Pt, even under high CO_2 pressure. Methanol production with %FE of up to 10% for the first 5-10 C cm^{-2} can be reproducibly detected but only after *ca.* 1 hr of electrolysis.[17] As a result, only a small to negligible current enhancement is expected on the CV timescale (ms to s) for CO_2 reduction in the presence of ANH additives chemically similar to **1**.

The reduction processes for **1-4** under CO_2 are quasi-reversible, and show features of diffusion control (see Randles-Sevcik plots in SI, Figure S5) with no peak current

saturation observed, indicating that it is unlikely we are observing an electrocatalytic process on the CV timescale (Figure S4). In comparison, the current enhancement for **3-H$_2$** under CO_2 is five-fold larger in magnitude with a 25% increase in the total current passed under CO_2 compared to its parent ANH **3**. No current enhancement above the background currents was observed for **4-H$_2$** under CO_2, similar to **4**.

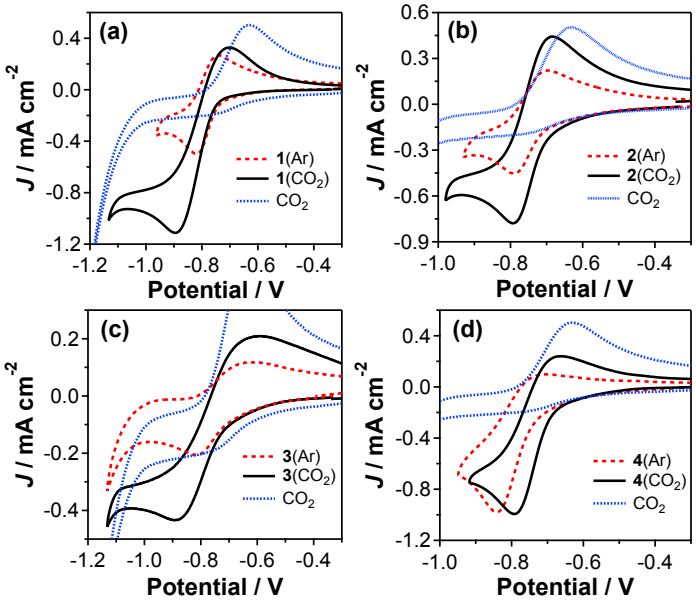

Figure 3. CVs 1 atm CO_2 (black); under Ar in acid (red); and CO_2 alone (1 atm, blue) for 10 mM of (a) **1**, pH = 5.5; (b) **2**, pH = 5.3; (c) **3**, pH = 5.2; (d) **4**, pH = 5.7. ν = 100 mV/s; 0.1 M $LiClO_4$, CH_3CN/H_2O (40% v/v), Pt disc; *E* vs $Fc^{0/+}$.

Given the electrode dependence of the %FEs for CO_2 reduction by ANHs and the absence of product formation by DHPs both without any applied potential or at RVC electrodes at lower $E_{applied}$ (-0.75 V), a strictly solution-based DHP mechanism for CO_2 reduction appears unlikely.[22,45] Lessio *et al.* recently established that a surface-bound 2-pyridinyl radical formed via transfer of photoexcited electrons from p-GaP to **[1-H]**$^+$ is thermodynamically feasible *in silico*, and calculated to be more reactive than the more stable surface-adsorbed DHP **[1-H$_2$]$_{ads}$** (Figure 4a).[24] Both are proposed as competent intermediates in ANH-mediated photoelectrochemical CO_2 reduction at p-GaP.

In our system, reactivity via surface-adsorbed $\mathbf{[3\text{-}H_2]_{ads}}$ directly does not account for the appearance of a reductive event in CVs of $\mathbf{3\text{-}H_2}$ under CO_2 (Figure 2b). Formation of a surface-bound DHP-derived radical ($DHP^{\bullet}_{ads}$; Figure 4b) via H_{ads} would explain the observation that different potentials are required for methanol and formate production in bulk electrolyses of DHPs $\mathbf{3\text{-}H_2}$ and $\mathbf{4\text{-}H_2}$ at RVC compared with Pt, as the surfaces require different potentials for H_{ads} formation, and that no homogenous reactivity occurs between $\mathbf{3\text{-}H_2}$/$\mathbf{4\text{-}H_2}$ and CO_2 in the absence of an electrode/potential.

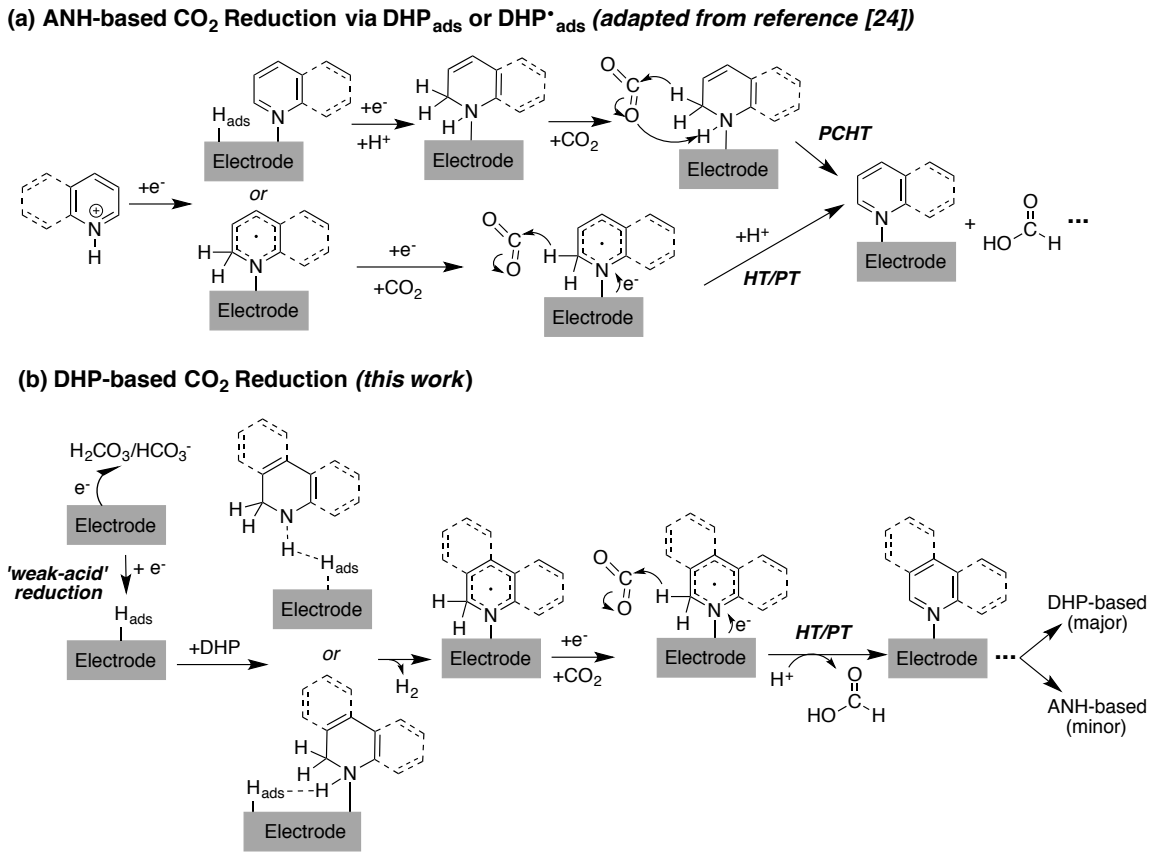

Figure 4. (a) Mechanism for ANH-based CO_2 reduction via DHP_{ads} or $DHP^{\bullet}_{ads}$ adapted from reference[24], PCHT = proton-coupled hydride transfer; (b) Proposed mechanism for observed CO_2 reduction in the presence of isolated DHP additives (this work) via formation of a surface-bound DHP-derived radical, $DHP^{\bullet}_{ads}$. HT = hydride transfer, PT = proton transfer. Only the initial reduction to HCOOH is illustrated, with subsequent steps leading to CH_3OH formation occurring in a similar fashion.

The mechanism proposed in Figure 4 would account for all the components required to observe methanol production: **3-H$_2$**, CO_2, a surface and a sufficiently reducing potential. Participation of H_{ads} (formed via 'weak-acid reduction' of carbonic acid in solution, as observed in the background current of CO_2 alone, Figure 2b)[44] accounts for the difference in potential required for methanol production at RVC vs Pt. CO_2 reduction is postulated to then occur via hydride transfer from the DHP-derived surface species, potentially stabilized by surface-organized waters,[22] followed by proton transfer from the acidic solution completing the initial reduction to formic acid. Bulk electrolyses of ANHs under CO_2 in dry, acidified CH_3CN at RVC and Pt electrodes resulted in no observable CO_2 reduction products, indicating a critical role for water in the reduction mechanism.

The formation of H_{ads} also appears to be critical to the activity of ANH additives and we cannot distinguish here a PCHT mechanism[27] or reactivity of a surface-bound DHP_{ads} or DHP-derived radical generated via H_{ads}, as proposed by Carter.[24] The decrease in %FE of the ANHs moving from Pt to RVC could result from increased ANH adsorption on RVC surfaces, though only **4** was observed to form a noticeable film after electrolysis under CO_2 at Pt surfaces and after one CV cycle at GCEs (Figure S6). A poisoning effect at high concentrations of **1** on $CuInS_2$ has been attributed to formation of an pyridine adsorption layer that leads to increased resistance to mass transfer.[16]

In conclusion, we present here the first evidence for the participation of isolated dihydropyridine-type species in surface-dependent electrochemical CO_2 reduction. This is based on the following observations: (1) methanol and formic acid are generated in electrolyses of isolated DHPs **3-H$_2$** or **4-H$_2$** under 1 atm of CO_2 at both Pt and RVC electrodes; (2) CV and NMR studies show that the parent ANHs **3** and **4** are not

generated from the corresponding DHPs in appreciable amounts in the absence of CO_2, ruling out ANH-only mediated activity; (3) no homogeneous reactivity is observed between DHPs **3-H$_2$** or **4-H$_2$** and CO_2 in the absence of an electrode surface/applied potential; and (4) DHP **3-H$_2$** exhibits an electrode dependence (Pt vs RVC) on the $E_{applied}$ required to observe methanol production, though not on the observed %FE.

The ability to carry out electrochemical CO_2 to methanol conversion using carbon-based electrodes instead of precious metals such as Pt or Pd is an important milestone for the scaleability of reduction schemes employing DHP or ANH additives.[46-48] Consistent with previous studies on **1**, however, the overall yields of reduced organic products in our experiments remain sub-stoichiometric, even in reactions mediated by pre-formed DHPs. Moreover, we did not observe evidence of electrochemical generation of DHP **3-H$_2$** from ANH **3**. These experimental findings will hopefully motivate better understanding of the mechanism of multi-H^+/e^- processes occurring in CO_2 electrochemical reduction in the presence of simple organic additives, and lead to the improvements in turnover numbers, for example, by targeting biomimetic hydride shuttles capable of cooperative interactions with electrode surfaces and electric potentials.[24,49-51]

ASSOCIATED CONTENT

Supporting Information. Full experimental details, supporting figures and tables; NMR spectra, GC and LC traces from bulk electrolysis samples (PDF). The Supporting Information is available free of charge on the ACS Publications website.

AUTHOR INFORMATION

*david.herbert@umanitoba.ca

Funding Sources

The Natural Sciences Engineering Research Council of Canada is gratefully acknowledged for a Discovery Grant to DEH (RGPIN-2014-03733) and a CGS-M Fellowship (PKG), as is the University of Manitoba for start-up funding (DEH) and GETS (PKG) support.

ACKNOWLEDGMENT

We thank Prof. Gregg Tomy for access to a LC-MS; MCAL (Dr. Tom Ward) for access to a GC-MS and GC-FID; Dr. Kirk Marat for assistance with NMR solvent suppression; and Thor Halldorson for helping develop a LC-MS method.

REFERENCES

(1) Hammarstrom, L.; Hammes-Schiffer, S. Artificial Photosynthesis and Solar Fuels. *Acc. Chem. Res.* **2009**, *42*, 1859-1860.

(2) Kumar, B.; Llorente, M.; Froehlich, J.; Dang, T.; Sathrum, A.; Kubiak, C. P. Photochemical and Photoelectrochemical Reduction of CO_2. *Annu. Rev. Phys. Chem.* **2012**, *63*, 541-569.

(3) Seshadri, G.; Lin, C.; Bocarsly, A. B. A New Homogeneous Electrocatalyst for the Reduction of Carbon Dioxide to Methanol at Low Overpotential. *J. Electroanal. Chem.* **1994**, *372*, 145-150.

(4) Barton Cole, E.; Lakkaraju, P. S.; Rampulla, D. M.; Morris, A. J.; Abelev, E.; Bocarsly, A. B. Using a One-Electron Shuttle for the Multielectron Reduction of CO_2 to Methanol: Kinetic, Mechanistic, and Structural Insights. *J. Am. Chem. Soc.* **2010**, *132*, 11539-11551.

(5) Barton Cole, E. E.; Baruch, M. F.; L'Esperance, R. P.; Kelly, M. T.; Lakkaraju, P. S.; Zeitler, E. L.; Bocarsly, A. B. Substituent Effects in the Pyridinium Catalyzed Reduction of CO_2 to Methanol: Further Mechanistic Insights. *Top. Catal.* **2015**, *58*, 15-22.

(6) Liao, K.; Askerka, M.; Zeitler, E. L.; Bocarsly, A. B.; Batista, V. S. Electrochemical Reduction of Aqueous Imidazolium on Pt(111) by Proton Coupled Electron Transfer. *Top. Catal.* **2015**, *58*, 23-29.

(7) Barton, E. E.; Rampulla, D. M.; Bocarsly, A. B. Selective Solar-Driven Reduction of CO_2 to Methanol Using a Catalyzed p-GaP Based Photoelectrochemical Cell. *J. Am. Chem. Soc.* **2008**, *130*, 6342-6344.

(8) Bocarsly, A. B.; Gibson, Q. D.; Morris, A. J.; L. Esperance, R. P.; Detweiler, Z. M.; Lakkaraju, P. S.; Zeitler, E. L.; Shaw, T. W. Comparative Study of Imidazole and Pyridine Catalyzed Reduction of Carbon Dioxide at Illuminated Iron Pyrite Electrodes. *ACS Catal.* **2012**, *2*, 1684-1692.

(9) Boston, D. J.; Xu, C.; Armstrong, D. W.; MacDonnell, F. M. Photochemical Reduction of Carbon Dioxide to Methanol and Formate in a Homogeneous System with Pyridinium Catalysts. *J. Am. Chem. Soc.* **2013**, *135*, 16252-16255.

(10) Jeon, J. H.; Mareeswaran, P. M.; Choi, C. H.; Woo, S. I. Synergism Between CdTe Semiconductor and Pyridine - Photoenhanced Electrocatalysis for CO_2 Reduction to Formic Acid. *RSC Adv.* **2014**, *4*, 3016-3019.

(11) Yuan, J.; Hao, C. Solar-Driven Photoelectrochemical Reduction of Carbon Dioxide to Methanol at $CuInS_2$ Thin Film Photocathode. *Sol. Energy Mater. Sol. Cells* **2013**, *108*, 170-174.

(12) White, J. L.; Baruch, M. F.; Pander, J. E., III; Hu, Y.; Fortmeyer, I. C.; Park, J. E.; Zhang, T.; Liao, K.; Gu, J.; Yan, Y. *et al.* Light-Driven Heterogeneous Reduction of Carbon Dioxide: Photocatalysts and Photoelectrodes. *Chem. Rev.* **2015**, *115*, 12888-12935.

(13) Costentin, C.; Canales, J. C.; Haddou, B.; Savéant, J.-M. Electrochemistry of Acids on Platinum. Application to the Reduction of Carbon Dioxide in the Presence of Pyridinium Ion in Water. *J. Am. Chem. Soc.* **2013**, *135*, 17671-17674.

(14) Savéant, J.-M.; Tard, C. Attempts To Catalyze the Electrochemical CO_2-to-Methanol Conversion by Biomimetic $2e^- + 2H^+$ Transferring Molecules. *J. Am. Chem. Soc.* **2016**, *138*, 1017-1021.

(15) Portenkirchner, E.; Enengl, C.; Enengl, S.; Hinterberger, G.; Schlager, S.; Apaydin, D.; Neugebauer, H.; Knoer, G.; Sariciftci, N. S. A Comparison of Pyridazine and Pyridine as Electrocatalysts for the Reduction of Carbon Dioxide to Methanol. *ChemElectroChem* **2014**, *1*, 1543-1548.

(16) Yuan, J.; Zheng, L.; Hao, C. Role of Pyridine in Photoelectrochemical Reduction of CO_2 to Methanol at a $CuInS_2$ Thin Film Electrode. *RSC Adv.* **2014**, *4*, 39435-39438.

(17) Rybchenko, S. I.; Touhami, D.; Wadhawan, J. D.; Haywood, S. K. Study of Pyridine-Mediated Electrochemical Reduction of CO_2 to Methanol at High CO_2 Pressure. *ChemSusChem* **2016**, *9*, 1660-1669.

(18) Morris, A. J.; McGibbon, R. T.; Bocarsly, A. B. Electrocatalytic Carbon Dioxide Activation: The Rate-Determining Step of Pyridinium-Catalyzed CO_2 Reduction. *ChemSusChem* **2011**, *4*, 191-196.

(19) Lucio, A. J.; Shaw, S. K. Pyridine and Pyridinium Electrochemistry on Polycrystalline Gold Electrodes and Implications for CO_2 Reduction. *J. Phys. Chem. C* **2015**, *119*, 12523-12530.

(20) Keith, J. A.; Carter, E. A. Theoretical Insights into Electrochemical CO_2 Reduction Mechanisms Catalyzed by Surface-Bound Nitrogen Heterocycles. *J. Phys. Chem. Lett.* **2013**, *4*, 4058-4063.

(21) Keith, J. A.; Carter, E. A. Electrochemical Reactivities of Pyridinium in Solution: Consequences for CO_2 Reduction Mechanisms. *Chem. Sci.* **2013**, *4*, 1490-1496.

(22) Lim, C.-H.; Holder, A. M.; Hynes, J. T.; Musgrave, C. B. Reduction of CO_2 to Methanol Catalyzed by a Biomimetic Organo-Hydride Produced from Pyridine. *J. Am. Chem. Soc.* **2014**, *136*, 16081-16095.

(23) Marjolin, A.; Keith, J. A. Thermodynamic Descriptors for Molecules That Catalyze Efficient CO_2 Electroreductions. *ACS Catal.* **2015**, *5*, 1123-1130.

(24) Lessio, M.; Senftle, T. P.; Carter, E. A. Is the Surface Playing a Role during Pyridine-Catalyzed CO_2 Reduction on p-GaP Photoelectrodes? *ACS Energy Lett.* **2016**, *1*, 464-468.

(25) Yan, Y.; Zeitler, E. L.; Gu, J.; Hu, Y.; Bocarsly, A. B. Electrochemistry of Aqueous Pyridinium: Exploration of a Key Aspect of Electrocatalytic Reduction of CO_2 to Methanol. *J. Am. Chem. Soc.* **2013**, *135*, 14020-14023.

(26) Zeitler, E. L.; Ertem, M. Z.; Pander, J. E., III; Yan, Y.; Batista, V. S.; Bocarsly, A. B. Isotopic Probe Illuminates the Role of the Electrode Surface in Proton Coupled Hydride Transfer Electrochemical Reduction of Pyridinium on Pt(111). *J. Electrochem. Soc.* **2015**, *162*, H938-H944.

(27) Ertem, M. Z.; Konezny, S. J.; Araujo, C. M.; Batista, V. S. Functional Role of Pyridinium during Aqueous Electrochemical Reduction of CO_2 on Pt(111). *J. Phys. Chem. Lett.* **2013**, *4*, 745-748.

(28) Minimal CH_3CN was required to dissolve **3**/**4** in water, and so for consistency the same solvent ratio was used all compounds. $LiClO_4$ chosen as the electrolyte due to its ability to dissolve in aqueous/non-aqueous mixtures.

(29) In our experimental set-up, %FE for hydrogen (H_2) was not determined as CO_2 is bubbled through the solution continuously.

(30) Lanning, J. A.; Chambers, J. Q. Voltammetric Study of the Hydrogen Ion/Hydrogen Couple in Acetonitrile/Water Mixtures. *Anal. Chem.* **1973**, *45*, 1010-1016.

(31) Lebegue, E.; Agullo, J.; Morin, M.; Bélanger, D. The Role of Surface Hydrogen Atoms in the Electrochem Reduction of Pyridine and CO_2 in Aqueous Electrolyte. *ChemElectroChem* **2014**, *1*, 1013-1017.

(32) Gennaro, A.; Isse, A. A.; Vianello, E. Solubility and Electrochemical Determination of CO_2 in Some Dipolar Aprotic Solvents. *J. Electroanal. Chem. Interfac. Electrochem.* **1990**, *289*, 203-215.

(33) Groenenboom, M. C.; Saravanan, K.; Zhu, Y.; Carr, J. M.; Marjolin, A.; Faura, G. G.; Yu, E. C.; Dominey, R. N.; Keith, J. A. Structural and Substituent Group Effects on Multielectron Standard Reduction Potentials of Aromatic N-Heterocycles. *J. Phys. Chem. A* **2016**, *120*, 6888–6894.

(34) pKa's in CH_3CN/H_2O were experimentally determined. See SI.

(35) Maksić, Z. B.; Barić, D.; Müller, T. Clar's Sextet Rule Is a Consequence of the σ-Electron Framework. *J. Phys. Chem. A* **2006**, *110*, 10135-10147.

(36) Chen, Q.-A.; Gao, K.; Duan, Y.; Ye, Z.-S.; Shi, L.; Yang, Y.; Zhou, Y.-G. Dihydrophenanthridine: A New and Easily Regenerable NAD(P)H Model for Biomimetic Asymmetric Hydrogenation. *J. Am. Chem. Soc.* **2012**, *134*, 2442-2448.

(37) Lu, L.-Q.; Li, Y.; Junge, K.; Beller, M. Iron-Catalyzed Hydrogenation for the In Situ Regeneration of an NAD(P)H Model: Biomimetic Reduction of α-Keto-/α-Iminoesters. *Angew. Chem., Int. Ed.* **2013**, *52*, 8382-8386.

(38) Shul, G.; Weissmann, M.; Bélanger, D. Electrochemical Formation of an Ultrathin Electroactive Film from 1,10-Phenanthroline on a Glassy Carbon Electrode in Acidic Electrolyte. *Langmuir* **2014**, *30*, 6612-6621.

(39) Shul, G.; Weissmann, M.; Bélanger, D. Electrochemical Characterization of Glassy Carbon Electrode modified with 1,10-Phenanthroline Groups by Two Pathways: Reduction of the Corresponding Diazonium Ions and Reduction of Phenanthroline. *Electrochim. Acta* **2015**, *162*, 146-155.

(40) Lessio, M.; Riplinger, C.; Carter, E. A. Stability of Surface Protons in Pyridine-Catalyzed CO_2 Reduction at p-GaP Photoelectrodes. *Phys. Chem. Chem. Phys.* **2016**, *18*, 26434-26443.

(41) Senftle, T. P.; Lessio, M.; Carter, E. A. Interaction of Pyridine and Water with the Reconstructed Surfaces of GaP(111) and CdTe(111) Photoelectrodes: Implications for CO_2 Reduction. *Chem. Mater.* **2016**, *28*, 5799-5810.

(42) Chen, L. D.; Urushihara, M.; Chan, K.; Nørskov, J. K. Electric Field Effects in Electrochemical CO_2 Reduction. *ACS Catalysis* **2016**, *6*, 7133-7139.

(43) Oxidative cycling was only conducted in survey CV scans, and was not performed prior to bulk electrolysis experiments of the DHP samples.

(44) Peroff, A. G.; Weitz, E.; Van Duyne, R. P. Mechanistic Studies of Pyridinium Electrochemistry: Alternative Chemical Pathways in the Presence of CO_2. *Phys. Chem. Chem. Phys.* **2016**, *18*, 1578-1586.

(45) Lim, C.-H.; Holder, A. M.; Hynes, J. T.; Musgrave, C. B. Catalytic Reduction of CO_2 by Renewable Organohydrides. *J. Phys. Chem. Lett.* **2015**, *6*, 5078-5092.

(46) Froehlich, J. D.; Kubiak, C. P. Homogeneous CO_2 Reduction by Ni(cyclam) at a Glassy Carbon Electrode. *Inorg. Chem.* **2012**, *51*, 3932-3934.

(47) Yang, N.; Waldvogel, S. R.; Jiang, X. Electrochemistry of Carbon Dioxide on Carbon Electrodes. *ACS Appl. Mater. Interfaces* **2016**, *8*, 28357-28371.

(48) Chapovetsky, A.; Do, T. H.; Haiges, R.; Takase, M. K.; Marinescu, S. C. Proton-Assisted Reduction of CO_2 by Cobalt Aminopyridine Macrocycles. *J. Am. Chem. Soc.* **2016**, *138*, 5765-5768.

(49) Maurin, A.; Robert, M. Noncovalent Immobilization of a Molecular Iron-Based Electrocatalyst on Carbon Electrodes for Selective, Efficient CO_2-to-CO Conversion in Water. *J. Am. Chem. Soc.* **2016**, *138*, 2492-2495.

(50) Murase, M.; Kitahara, G.; Suzuki, T. M.; Ohta, R. Efficient Catalytic Electrode for CO_2 Reduction Realized by Physisorbing Ni(cyclam) Molecules with Hydrophobicity Based on Hansen's Theory. *ACS Appl. Mater. Interfaces* **2016**, *8*, 24315-24318.

(51) Lau, G. P. S.; Schreier, M.; Vasilyev, D.; Scopelliti, R.; Grätzel, M.; Dyson, P. J. New Insights Into the Role of Imidazolium-Based Promoters for the Electroreduction of CO_2 on a Silver Electrode. *J. Am. Chem. Soc.* **2016**, *138*, 7820-7823.